<u>Supplementary material</u>

Self-assembled membrane with excellent antifouling performance for enhanced treatment of petrochemical wastewater

Kexuan Gao[a], Yu Yang[a]*, Nigel J.D. Graham[b], Ying Zhang[a], Yilin Jiang[a], Cheng Duan[a], Ao Li[a], Qianqian Zhang[a], Xiaoqiang An[c], Li-an Hou[a]*

[a] State Key Laboratory of Water Environment Simulation, School of Environment, Beijing Normal University, Beijing 100875, China

[b]Department of Civil and Environmental Engineering, Imperial College London, South Kensington Campus, London SW7 2AZ, UK

[c] Center for Water and Ecology, State Key Joint Laboratory of Environment Simulation and Pollution Control, School of Environment, Tsinghua University, Beijing 100084, China

* Corresponding author.

E-mail address: yangyu@bnu.edu.cn *(Yu Yang)*; houla@cae.cn *(Li-an Hou)*

This supporting information contains the following:

Text

Text S1

Bragg's law is shown by the following expression [1]:

$$\lambda = 2d\sin(\theta) \quad \text{(S-1)}$$

where λ is the wavelength of the X-ray beam (0.154 nm), d is the distance between adjacent GO flakes, and θ is the diffraction angle of the peak.

Text S2

Membrane resistance, fouling reversibility, and the resistance to cleaning of various foulants are listed in Table S4. High velocity flushing for 15 min was adopted as a typical physical cleaning method, while chemical cleaning methods were optimized according to the flux recovery rates (*F*rrs). As shown in Table S5, the *F*rr rose from 87%

to 93%, when NaOH concentration increased from 0.1 wt% to 0.5 wt%. NaOH solution facilitated the deprotonation of functional groups in organic foulants, and loosened the fouling layer through generating repulsion forces between the foulants and the fouling layer. To further enhance the chemical cleaning efficiency, NaClO and 0.1 wt% NaOH were applied as an oxidant to remove organic pollutants accumulated on the membrane surface and inside membrane pores, which achieved 95% and 98% removal when its concentration reached 0.05 wt % and 0.1 wt%, respectively.

Text S3

The corresponding parameters K_c and K_i of the complete blockage model and the intermediate blockage model are expressed as follows [2, 3]：

$$K_c = \frac{3\rho_m X_m}{4\rho_s \alpha_p \psi} \quad \text{(S-2)}$$

$$K_i = \frac{3\rho_m X_m}{4\rho_s \alpha_p \psi} \quad \text{(S-3)}$$

Where, K_c (m^{-1}) is a constant parameter related to the completely blocked model; K_i (m^{-1}) is a constant parameter related to the intermediate blocking model; ρ_m is the density of the solution on the membrane surface; X_m is the mass fraction of solute on the membrane surface; ρ_s is the density of the solute; α_p is the molecular radius of the solute; ψ is the shape factor of the solute molecule.

Text S4

According to the resistance-in-series models, the total membrane resistance (R_t) is principally divided into reversible (R_r) and irreversible (R_{ir}) membrane resistances [4]. The membrane resistances, fouling reversibility, and the resistance to cleaning of various foulants are listed in Table S4. The GO/PVDF membrane exhibited 50% lower irreversible fouling resistance (R_{irr}) than the PVDF membrane when treating SPW and SPW-I. The superior fouling resistance performance of the GO/PVDF membrane was even more distinct in the treatment of RPW, where the flux recovery rate reached 92.41%, substantially higher than that of the PVDF membrane (73.33%), and the R_{irr} was reduced by 70% (Table S4). According to the analysis of membrane resistance under different wastewater conditions, the modified GO/PVDF membrane possessed better anti-fouling performance than the pristine PVDF membrane, which was partially attributed to the enhanced hydrophilicity and negatively charged surface of the modified membrane.

Text S5

Cost accounting and study limitations

The manufacture and operation of the modified membrane per square meter served as the basis for the preliminary costing of the GO/PVDF membrane for petrochemical wastewater treatment; the assumed values included in the cost analysis were those valid for June 2024 values. The membrane preparation cost was made up of material and reagent consumption costs, while the operating cost was principally the electrical power required by the process and the chemical costs associated with membrane cleaning. The costs for industrial raw materials such as GO, PVDF, EDA, $NaHSO_3$, KOH, H_2SO_4, and trimesoyl chloride, are given in the SI (Table S11). The cost per square meter of the GO/PVDF membrane was calculated to be approximately $31.217. Based on the long-term operational parameters established in this study, the effective membrane area was

24 cm^2, and the daily capacity of the reactor was 10.31 m^3 at a permeate flux of 179 LMH. The water supply pump was a diaphragm booster pump capable of running 20 membrane modules with a motor power of 0.024 kW. The average daily electricity price for large industries in Beijing's urban region was assumed to be approximately 0.11 USD / kWh. In summary, the operational cost of the GO/PVDF membrane system for treating petrochemical effluent was approximately \$31.2 m^{-3}. Thus, it can be seen that the main item of cost of the membrane system was the membrane itself, and thus, in subsequent research studies, emphasis should be placed on further surface modification of the membrane to alleviate fouling and improve the membrane service life, in order to reduce the cost of the membrane treatment process.

Petrochemical wastewater is a typical industrial wastewater that contains high concentrations of organic pollutants that are toxic and harmful to plants, animals and ecosystems. A significant limitation of this study is the wide variation in water quantity in petrochemical wastewaters. Production fluctuations in petrochemical operations, such as starting and stopping, maintenance, and changes in the original source, can cause substantial changes in water quantity, as well as pollutant content and properties, which increase the load on the wastewater treatment facilities. Although this study did not explicitly model these changes, further studies can be undertaken subsequently to demonstrate the suitability and advantages of the novel membrane for other types of petrochemical wastewaters.

Tables

Table S1. Water quality of real petrochemical wastewater (RPW)

Quality parameters		unit	value
pH		—	6.6
Conductivity		µS/cm	1668
Concentration of principal ions	SO_4^{2-}	mg/L	422.3
	Na^+	mg/L	382.0
	Cl^-	mg/L	125.1
	Ca^{2+}	mg/L	52.8
	NH_4^+-N	mg/L	13.5
	K^+	mg/L	12.2
	Mg^{2+}	mg/L	11.3
	NO_3^-	mg/L	0.1
COD		mg/L	247.7
Concentration of main organic components	benzene	%	45.8
	Toluene	%	25.4
	M-xylene	%	4.8
	P-xylene	%	3.7
	Methyl tert-butyl ether	%	2.9
	Ethylbenzene	%	2.1
	Pentadecane	%	1.7
	Dimethyl disulfide	%	1.2
	Octamethyl cyclo tetrasiloxane	%	1.2

Table S2. Compositions of synthetic petrochemical wastewater (SPW) and synthetic petrochemical wastewater with co-existing ions (SPW-I)

	Compositions	Formula	Concentration（ppm）
SPW	Benzene	C_6H_6	58
	Toluene	C_7H_8	32
SPW-I	Benzene	C_6H_6	58
	Toluene	C_7H_8	32
	Ammonium sulfate	$(NH_4)_2SO_4$	7.5
	Potassium chloride	KCl	10
	Calcium chloride	$CaCl_2 \cdot 2H_2O$	50
	Sodium sulfate	Na_2SO_4	200
	Magnesium sulfate	$MgSO_4$	10

Table S3. The water flux, contact angle and zeta potential of PVDF, GO/PVDF-5 and GO/PVDF-10 membranes.

	pure water permeability (LMH*/bar)	water contact angle	Zeta potential (mV)
PVDF	385~425	78.5 ± 2°	-36.6 ± 1
GO/PVDF-5	226~234	70.5 ± 3°	-40.1 ± 1.4
GO/PVDF-10	179~194	66 ± 2°	-46.8 ± 0.5

*LMH – $L/m^2 \cdot h$

Table S4. Flux recovery rates and membrane fouling ratios of GO/PVDF-10 and PVDF membranes in treating synthetic petrochemical wastewater (SPW), synthetic petrochemical wastewater with co-existing ions (SPW-I), and real petrochemical wastewater (RPW).

	SPW		SPW-I		RPW	
	PVDF	GO/PVDF	PVDF	GO/PVDF	PVDF	GO/PVDF
F_{rr} (%)	83.82	89.19	82.20	89.39	73.33	92.41

R_t (%)	28.53	18.92	28.73	19.70	32.00	40.60
R_r (%)	7.35	8.11	5.93	9.09	5.33	33.00
R_{ir} (%)	21.18	10.81	22.80	10.61	26.67	7.59

Table S5. The percent composition from XPS.

	C-F	C=O	C-C	C=C
GO/PVDF	9.83	39.00	23.49	27.05
Ultrasound	29.67	25.12	25.82	26.04
NaOH	43.91	18.56	31.08	16.54
NaClO	16.59	17.31	19.61	30.38

Table S6. Flux recovery rates of GO/PVDF-10 achieved by chemical cleaning.

	NaOH (0.1 wt%)	NaOH (0.5 wt%)	NaClO (0.05 wt%) + NaOH (0.1 wt%)	NaClO (0.1 wt%) + NaOH (0.1 wt%)
F_{rr} (%)	87±2	93±1	95±1	98±1.5

Table S7. Fitting parameters of Hermia's blocking models for GO/PVDF-10 membrane filtering organic, ion-containing simulated wastewater and petrochemical wastewater.

	First 3 h Filtration				Filtration cycle before the last chemical cleaning							
	Complete Blocking Model		Intermediate Blocking Model		Complete Blocking Model		Intermediate Blocking Model		Standard Blocking Model		Cake Blocking Model	
	R^2	K_c	R^2	K_i	R^2	K_c	R^2	K_i			R^2	K_{ca}
SPW	0.9894	1.38E-05	0.9898	1.45E-05	0.9889	1.55E-05	0.9892	1.62E-05				
SPW-I	0.9948	4.67E-05	0.9949	4.37E-05	0.8244	2.50E-05	0.8265	2.50E-05				
RPW	0.90864	3.47E-04	0.91532	3.69E-04	0.94026	1.38E-04	0.96548	1.74E-04	—	—	0.9410	5.8002

Table S8. Comparison with PVDF-modified membranes reported in the literature.

Membrane	Preparation Method	Water flux ($L/m^2·h$)	Pollutant (Rejection%)	Running time	Ref.
PVDF/GO/LiCl	Phase inversion	61.9	Rhodamine B (67.8%)	80 min	[5]
PVDF/GO/PVP	Phase inversion	104.3	BSA (85%)	/	[6]
PVDF/PAA/TiO2	Grafting from	68	Whey solution (87%)	3 h	[7]
PVDF/PVP	Grafting	155	Oil (98%)	1 h	[8]
PVDF/P-ND	Phase inversion	121.8±2.1	COD (94.2%)		[9]
PVDF/MWCNT	Phase inversion	137	BSA (99%) RG19 Dye (97%)	1h	[10]
PZGS-Mx-PVDF	Phase inversion	7.6/26.3	Oil (99.3/98.1%)	/	[11]
PVDF/PANI	Phase inversion	47	Dye (85%)	450h	[12]
PVDF	TIPS	65	Water Turbidity (98.56%)	480h	[13]
GO/PVDF	LBL assembly	179~194	COD (95.3%)	445h	This work

Table S9. Water contact angle and zeta potential of PVDF and GO/PVDF membranes before and after physical/chemical cleaning.

	Contact angle (°)	Zeta potential (mV)

PVDF membrane	Before Cleaning	68±3	-12.33±0.5
	After physical Cleaning	68.5±1.5	-21.41±0.1
	After chemical Cleaning	85±3	-23.65±0.8
GO/PVDF membrane	Before Cleaning	64.5±2.5	-31.41±0.5
	After physical Cleaning	55±3.5	-37.04±0.2
	After chemical Cleaning	77.5±0.5	-46.66±0.5

Table S10. The effects of different NaClO cleaning concentrations on the properties of GO/PVDF membranes.

	Ultrasonic cleaning	Ultrasonic cleaning + 0.4 wt% NaClO	Ultrasonic cleaning + 0.3 wt% NaClO	Ultrasonic cleaning + 0.2 wt% NaClO
F_{rr} (%)	65.25	91.67	83.22	75.90
R_t (%)	39.88	-	-	-
R_r (%)	26.32	36.55	33.19	30.27
R_{ir} (%)	13.56	3.33	6.69	9.61

Table S11. Cost accounting per square meter of GO/PVDF membrane preparation.

Reagent/material	Unit price (USD)	Consumption	Expense (USD)
GO	5970 kg^{-1}	6.525 μg	0.0389
PVDF	24.42 m^2	1 m^2	24.42
EDA	1.64 kg^{-1}	0.25 kg	0.0082
$NaHSO_3$	0.29 kg^{-1}	0.104 kg	0.0006
KOH	0.89 kg^{-1}	0.04 kg	0.0007

H_2SO_4	0.0357 L^{-1}	0.2 mL	$1.43*10^{-7}$
N-hexane	0.88 L^{-1}	1 L	0.0176
Trimesoyl chloride	194 kg^{-1}	0.25 kg	0.97
NaOH	0.394 kg^{-1}	0.001 kg	$3.94*10^{-4}$
NaClO	0.066 kg^{-1}	0.0005 kg	$3.3*10^{-5}$

Figures

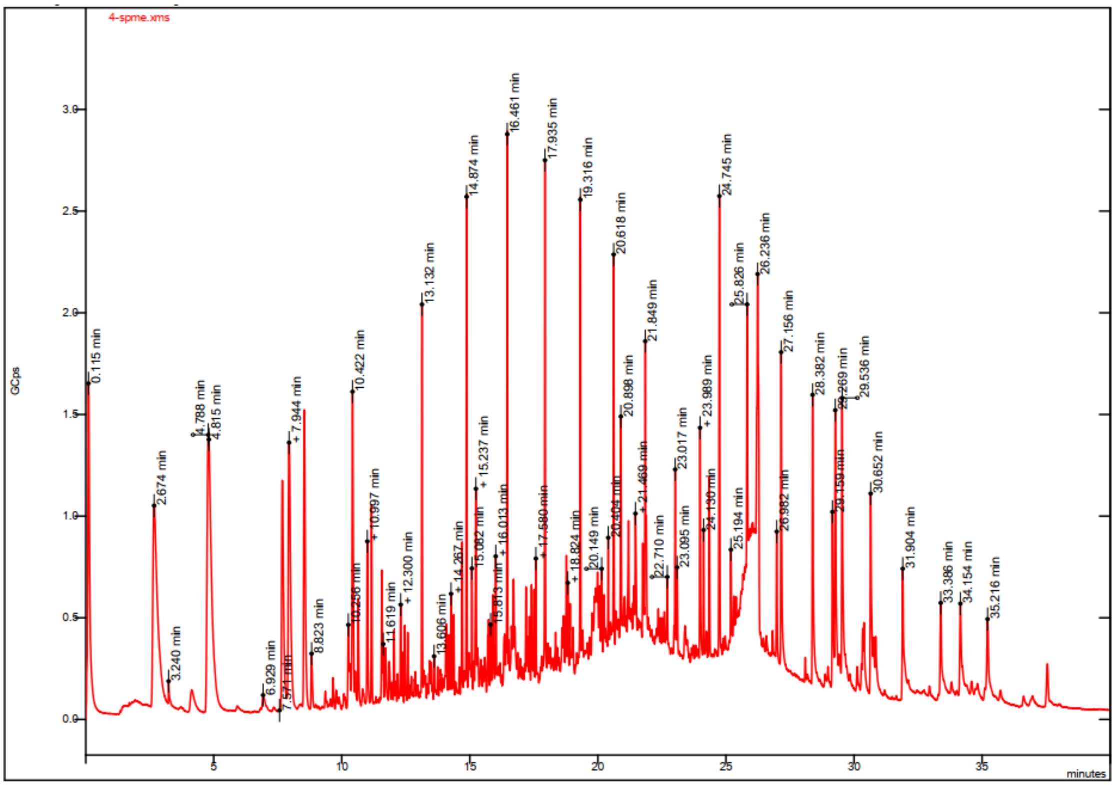

Fig. S1. GC-MS spectra of real petrochemical wastewater sample.

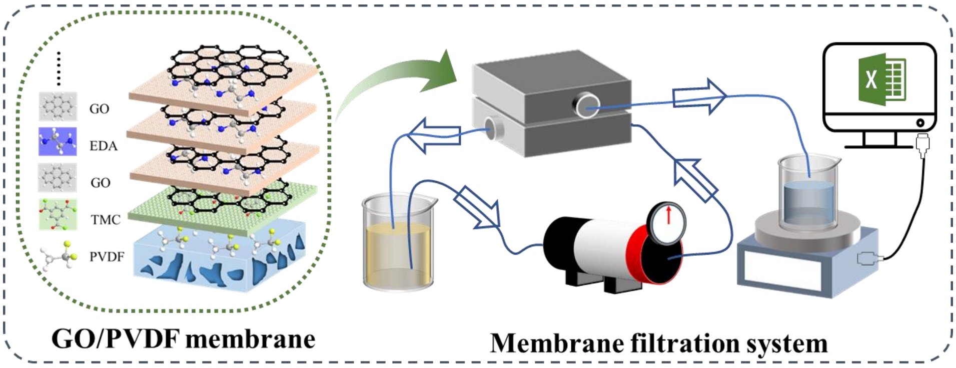

Fig. S2 Schematic diagram of membrane preparation process and membrane filtration system

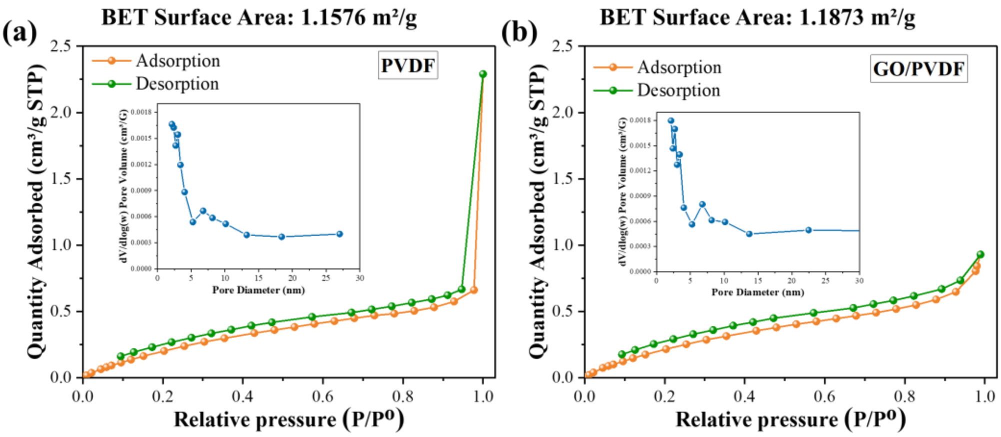

Fig. S3 Nitrogen sorption isotherms and corresponding pore size distribution (insert) of PVDF (a) and GO/PVDF (b) porous membrane.

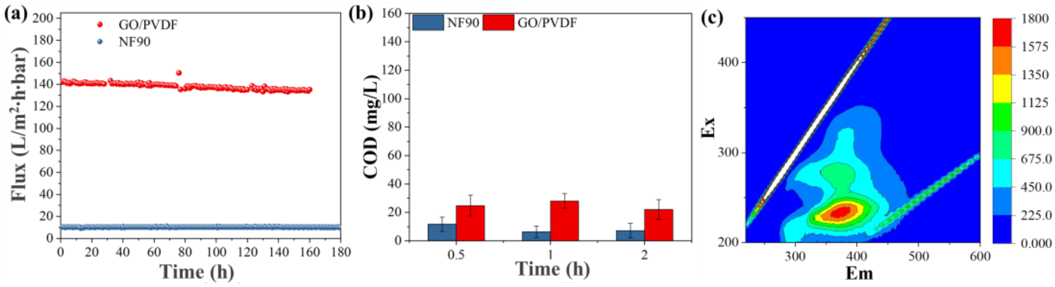

Fig. S4. Water flux (a) and effluent COD (b) of GO/PVDF-10 membrane and NF90 in the treatment of RPW, fluorescence EEM spectrum for RPW(c).

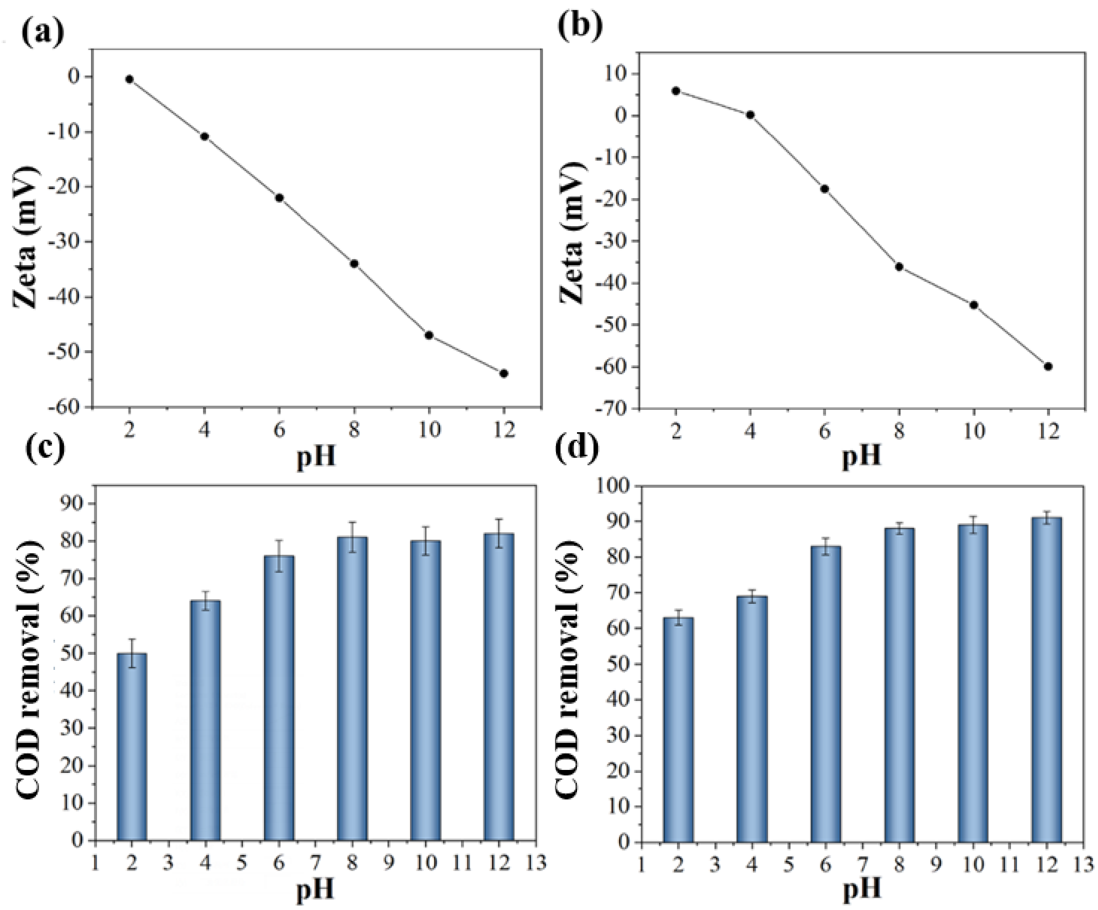

Fig. S5. Variation of zeta potential and COD removal of GO/PVDF-10 membrane (a,c) and NF90 membrane (b,d) with pH.

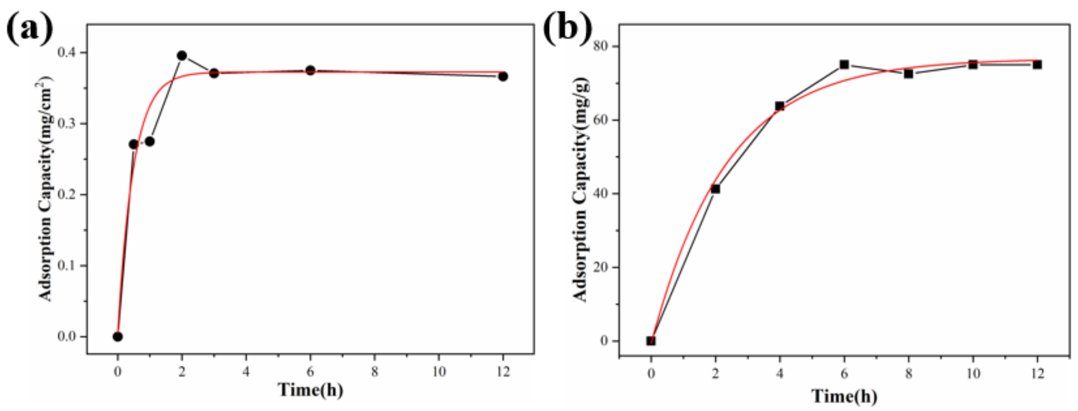

Fig. S6. The COD adsorption capacity for (a) GO/PVDF-10 membrane and (b) GO suspension (red lines indicate the fitting curve of the pseudo-first-order dynamics).

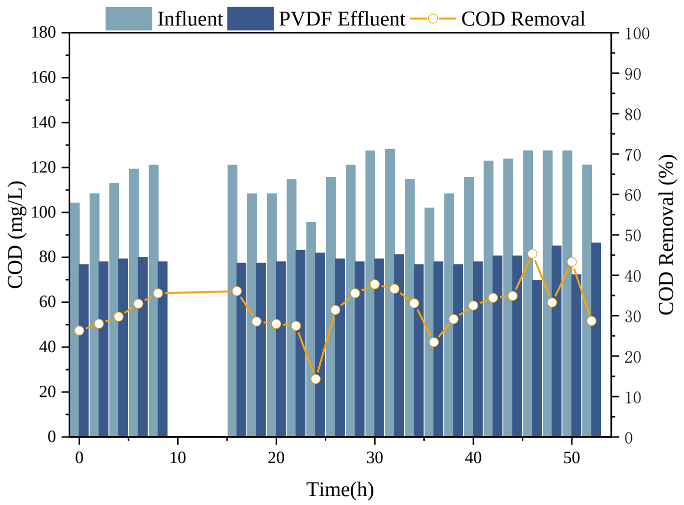

Fig. S7. Changes of COD in the filtration of simulated wastewater by PVDF membrane.

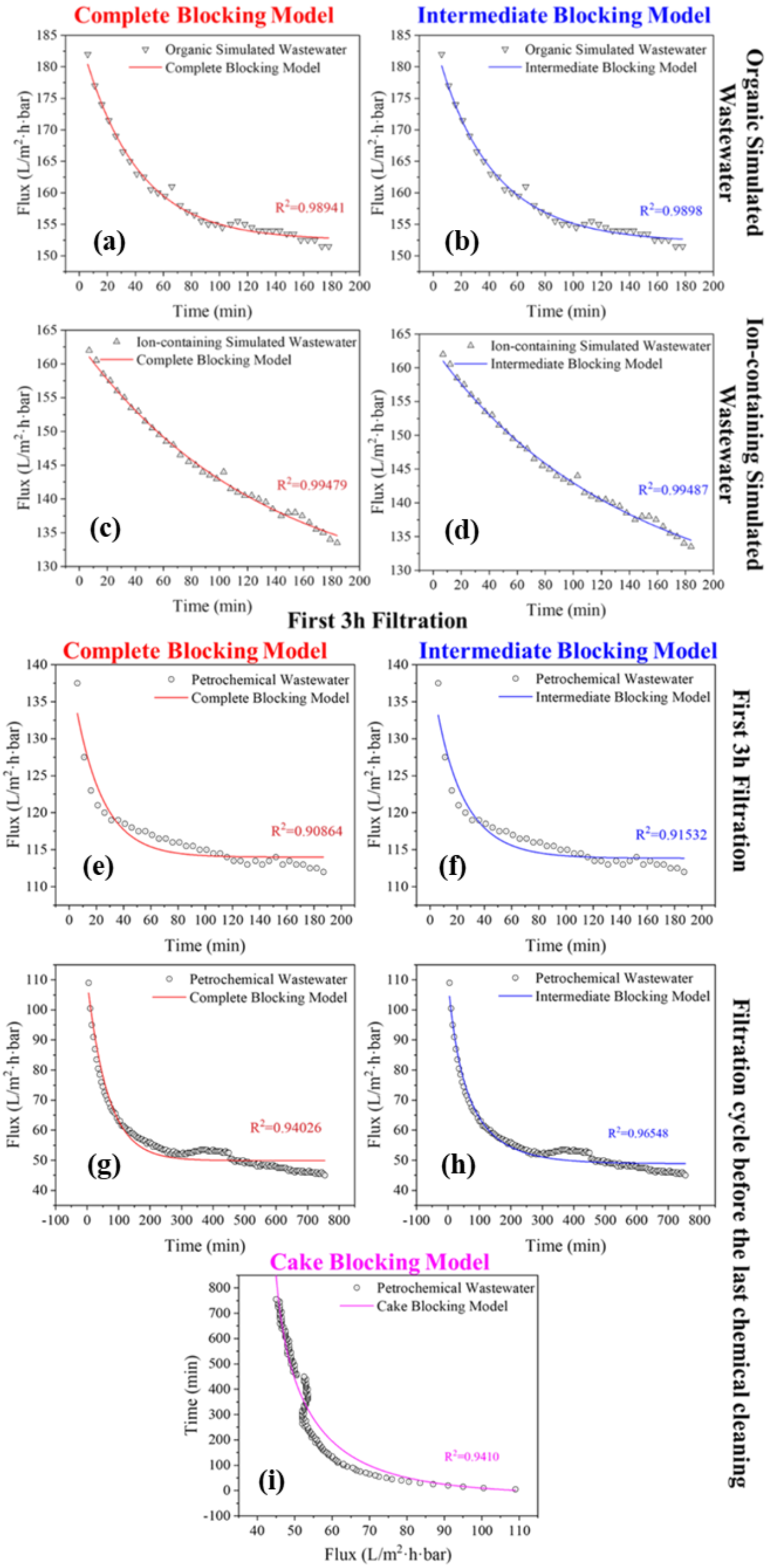

Fig. S8. Model fitted results of GO/PVDF-10 membrane treating organic simulated wastewater, ion-containing simulated wastewater and real petrochemical wastewater

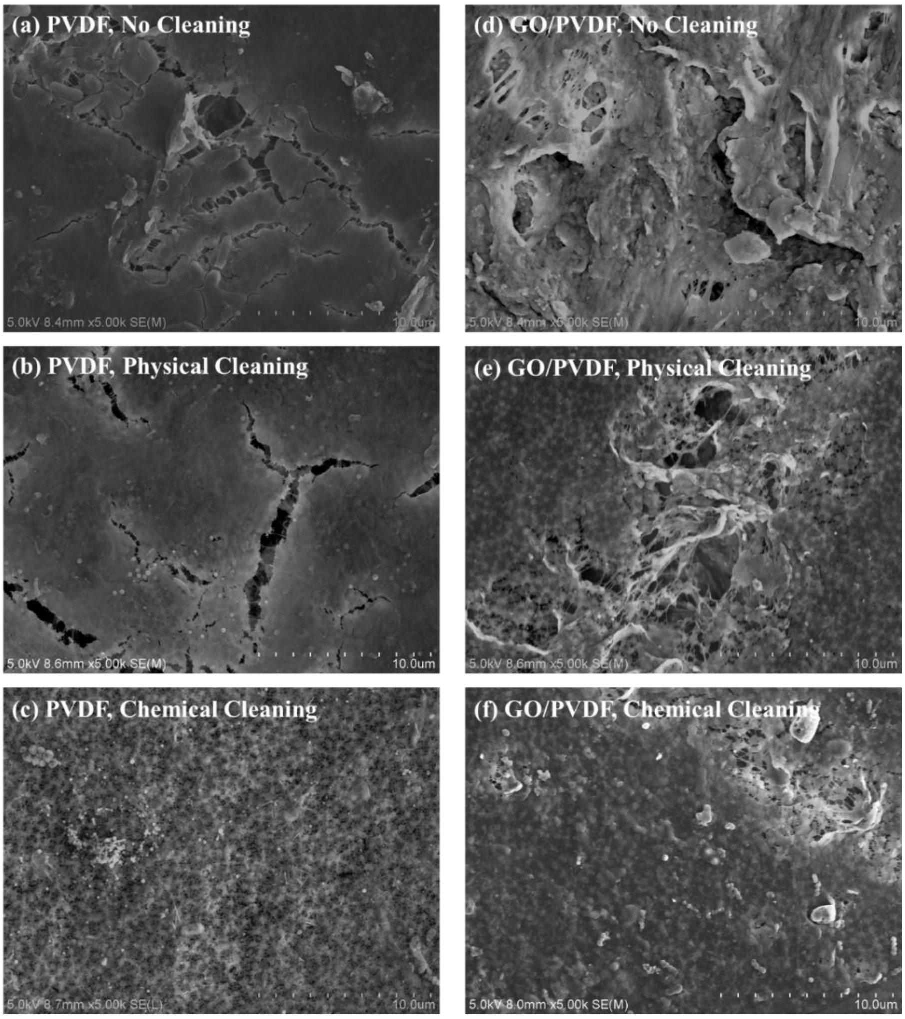

Fig. S9. SEM images of PVDF and GO/PVDF-10 membrane before and after physical or chemical cleaning.

References

[1] Zhang, T,Zhang, L-Z, Development of a MXene-based membrane with excellent anti-fouling for air humidification-dehumidification type desalination. *Journal of Membrane Science*, *641,* (2022) 119907. http://doi.org/https://doi.org/10.1016/j.memsci.2021.119907

[2] Vela, MCV,Blanco, SÁ,García, JL,Rodríguez, EB, Analysis of membrane pore blocking models adapted to crossflow ultrafiltration in the ultrafiltration of PEG. *Chemical Engineering Journal*, *149,* 1-3, (2009) 232-241. http://doi.org/https://doi.org/10.1016/j.cej.2008.10.027

[3] Gomes, MCS,Moreira, WM,Paschoal, SM,Sipoli, CC,Suzuki, RM,Sgorlon, JG,Pereira, NC, Modeling of fouling mechanisms in the biodiesel purification using ceramic membranes. *Separation and Purification Technology*, *269,* (2021) 118595. http://doi.org/https://doi.org/10.1016/j.seppur.2021.118595

[4] Li, Z,Li, X,Liu, Y,Zhou, Z,Ren, J,Lu, Z,Feng, J, Construction of sandwich-structured photocatalytic membranes to regulate the conversion of natural organic matter: Enhancement of anti-fouling performance. *Separation and Purification Technology*, *338,* (2024) 126588. http://doi.org/https://doi.org/10.1016/j.seppur.2024.126588

[5] Zhu, Z,Wang, L,Xu, Y,Li, Q,Jiang, J,Wang, X, Preparation and characteristics of graphene oxide-blending PVDF nanohybrid membranes and their applications for hazardous dye adsorption and rejection. *Journal of colloid and interface science*, *504,* (2017) 429-439. http://doi.org/10.1016/j.jcis.2017.05.068

[6] Chang, X,Wang, Z,Quan, S,Xu, Y,Jiang, Z,Shao, L, Exploring the synergetic effects of graphene oxide (GO) and polyvinylpyrrodione (PVP) on poly (vinylylidenefluoride)(PVDF) ultrafiltration membrane performance. *Applied Surface Science*, *316,* (2014) 537-548. http://doi.org/10.1016/j.apsusc.2014.07.202

[7] Madaeni, S,Zinadini, S,Vatanpour, V, A new approach to improve antifouling property of PVDF membrane using in situ polymerization of PAA functionalized TiO_2 nanoparticles. *Journal of membrane science*, *380,* 1-2, (2011) 155-162. http://doi.org/10.1016/j.memsci.2011.07.006

[8] Huang, X,Wang, W,Liu, Y,Wang, H,Zhang, Z,Fan, W,Li, L, Treatment of oily waste water by PVP grafted PVDF ultrafiltration membranes. *Chemical Engineering Journal*, *273,* (2015) 421-429. http://doi.org/10.1016/j.cej.2015.03.086

[9] Javadi, M,Jafarzadeh, Y,Yegani, R,Kazemi, S, PVDF membranes embedded with PVP functionalized nanodiamond for pharmaceutical wastewater treatment. *Chemical Engineering Research and Design*, *140,* (2018) 241-250. http://doi.org/10.1016/j.cherd.2018.10.029

[10] Gholami, S,Llacuna, JL,Vatanpour, V,Dehqan, A,Paziresh, S,Cortina, JL, Impact of a new functionalization of multiwalled carbon nanotubes on antifouling and permeability of PVDF nanocomposite membranes for dye wastewater treatment. *Chemosphere*, *294,* (2022) 133699. http://doi.org/10.1016/j.chemosphere.2022.133699

[11] Mansha, M,Salhi, B,Ali, S,Khan, SA,Baig, N, Novel procaine-based gemini zwitterion incorporated PVDF membranes for efficient treatment of oily wastewater. *Journal of Environmental Chemical Engineering*, *10,* 3, (2022) 107935. http://doi.org/10.1016/j.jece.2022.107935

[12] Nawaz, H,Umar, M,Nawaz, I,Ullah, A,Tauseef Khawar, M,Nikiel, M,Razzaq, H,Siddiq, M,Liu, X, Hybrid PVDF/PANI membrane for removal of dyes from textile wastewater. *Advanced Engineering Materials*, *24,* 5, (2022) 2100719. http://doi.org/10.1002/adem.202100719

[13] Zhang, Y,Yuan, Z,Bai, H,Zhao, L,He, L,Shi, C, A pilot-scale treatment of steel plant wastewater by PVDF hollow fiber ultrafiltration membrane with low packing density. *Separations*, *9,* 2, (2022) 37. http://doi.org/10.3390/separations9020037